ELSEVIER

Journal of Nuclear Materials 279 (2000) 293–300

journal of nuclear materials

www.elsevier.nl/locate/jnucmat

Mechanisms and kinetics of tempering in weldments of 9Cr–1Mo steel

M. Vijayalakshmi *, S. Saroja, R. Mythili, V. Thomas Paul, V.S. Raghunathan

Materials Characterisation Group, Metallurgy and Materials Group, Indira Gandhi Centre for Atomic Research, Kalpakkam 603 102, India

Received 8 February 1999; accepted 7 December 1999

Abstract

The microstructural mechanisms and the kinetics of the tempering process in an MMA welded 9Cr–1Mo steel have been studied in detail. Based on the microstructural studies of the various regions of the weldment tempered at different temperatures, three distinct mechanisms could be identified for the gradual softening observed in the weldments. A classification scheme has been proposed based on which the temperature regimes over which tempering proceeds through different mechanisms, have been rationalised. The kinetics of the tempering process have been studied using the temperature dependence of the rate of softening. The apparent activation energy of the tempering process is evaluated using an Arrhenius analysis and the corresponding rate-controlling process is identified as the diffusion of carbon in α-ferrite.

1. Introduction

The 'ferritics', in their wrought and welded conditions, are used as boilers and superheaters in the steam generator circuits of power industry. The 'ferritics' are chosen [1,2] to be the candidate materials for core component applications, in high power fast breeder nuclear reactors, due to their exceptionally high void swelling resistance. One of the important requirements of power industry is the stability of the properties and hence the microstructure, of the components, at the temperature of operation, throughout their lifetime. Therefore, it becomes essential to ensure that there is no degradation of long-term, high temperature properties, of not only the wrought materials, but also their weldments. The structure of weldments of ferritics is heterogeneous and the extent of heterogeneity depends [3,4] on the chemistry and the welding parameters. The modification of such heterogeneous structures at elevated temperatures, in turn, depends [5–7] on many parameters, like the structure and microchemistry of the initial phase, difference in the activity of the solutes in the different regions of the weldment, etc. Of the many changes that occur during exposure of the weldment to elevated temperatures, the present paper discusses the micromechanisms and the kinetics of the tempering of the weld region of the 9Cr–1Mo weldment.

The first part of the paper presents the modification of the microstructure of the weldment at high temperatures, which is responsible for the observed softening. A classification scheme to represent the temperature regimes with different softening mechanisms is proposed. The second part of the paper discusses the Arrhenius behaviour of the tempering process and the identification of the rate limiting process as the diffusion of interstitial carbon in α-ferrite.

2. Experimental

The weldments of 9Cr–1Mo steel were prepared from the normalised and tempered steel, supplied by M/s. Creusot Loire, France in the form of plates of 12.5

* Corresponding author. Tel.: +91-4114 40 306; fax: +91-4114 40 360/40 381.

E-mail address: mvl@igcar.ernet.in (M. Vijayalakshmi).

0022-3115/00/$ - see front matter
PII: S0022-3115(99)00289-5

mm thickness. The nominal composition of the steel supplied is given in Table 1. The weldments were prepared by multi-pass shielded metal arc process using basic coated electrodes. The welding parameters are given in Table 2. The post-weld heat treatment details and the specimen preparation details are given elsewhere [8]. Vicker's microhardness tests were carried out using Leitz Tester, using an applied load of 100 g. Optical microscopy was carried out using Reichert MeF2. Philips SEM 501 was used for the scanning electron microscopy observations and CM 200 with super ultra-thin window EDAX detector was used for the analytical transmission electron microscopy (ATEM). ATEM was carried out in thin foils and carbon extraction replicas, for the determination of the microchemistry of the secondary carbides.

3. Results and discussion

It has been shown [8] that the 'as welded' microstructure of 9Cr–1Mo weldments consists of distinct zones, the structure of which is sensitive to the distance of the regions from the 'heat source' during welding. These microstructural variations are found to originate from the differences in the thermal cycles each region is subjected to. Fig. 1(a) shows the microstructure of the three different zones of the weldment namely, weld, heat affected zone and the base metal. The weld region consists of only martensite, while there are a number of microstructural zones in the heat affected zone (HAZ), with the base metal having the normalised and tempered structure. As a consequence of the steep microstructural variations, the hardness of the various zones are distinctly different. Fig. 1(b) shows the three-dimensional representation of the variation in the hardness of the weldment. It is clear that the initial hardness of a region depends on the distance from the weld centre line.

Fig. 2 shows the variation of microhardness as a function of distance from the weld centre line of the weldments, tempered at different temperatures, for various durations. A gradual reduction in the hardness is observed with increase in the distance from the weld centre line. The variation in the microhardness of the weldment across the three different regions, like weld, HAZ and the base metal is larger at 823 K, unlike the other two temperatures. There is a significant reduction in the hardness of the weld close to the weld centre line after tempering at 823 K for 10 h. Such steep reductions are observed within a short time of 2 h, at the higher temperatures. There is no remarkable change in the microhardness values of the base metal for the different tempering times at the higher temperatures.

3.1. Microstructural modifications during exposure to elevated temperatures

The microstructural observations of the individual regions of the weldment, in the temperature range 823–1223 K, suggest that there are distinct processes that contribute to the gradual reduction in hardness with increase in the distance from the weld centre line.

The presence of laths after aging for 250 h at 823 K is shown in Fig. 3(a). Fig. 3(b)–(d) shows the micrographs of typical carbon extraction replica of the three regions, weld, HAZ and the base metal, aged at 823 K for 250 h. The retention of the lath structure, despite prolonged aging and the extensive precipitation of carbides are clearly seen, in all the three regions. Most of these carbides are found to be only $M_{23}C_6$, with a lower ratio of concentration of Cr to that of Fe, compared to M_2X (Fig. 3(e)), which is seen rarely in the base metal (arrow-marked in Fig. 3(d)).

Table 1
Nominal chemical composition of the 9Cr–1Mo steel used

Sl. no.	Chemical composition (w/o)				
	Cr	Mo	Si	C	Fe
1	8.24	0.96	0.19	0.07	Bal.

Table 2
Welding method and parameters

Sl. no.	Description	Value
1	Process	Manual metal arc
2	Pre-heat	200°C
3	Electrode	Basic coated 9Cr–1Mo electrodes
4	Composition of electrode in wt%	Cr – 8.9%, Mo – 0.98%, C – 0.12%, Mn and Si – 0.52%, P – 0.003%, S – 0.03%
5	Electrode diameter	3.15 mm
6	Arc voltage	22 V
7	Current	100–130 A
8	No. of passes	Four

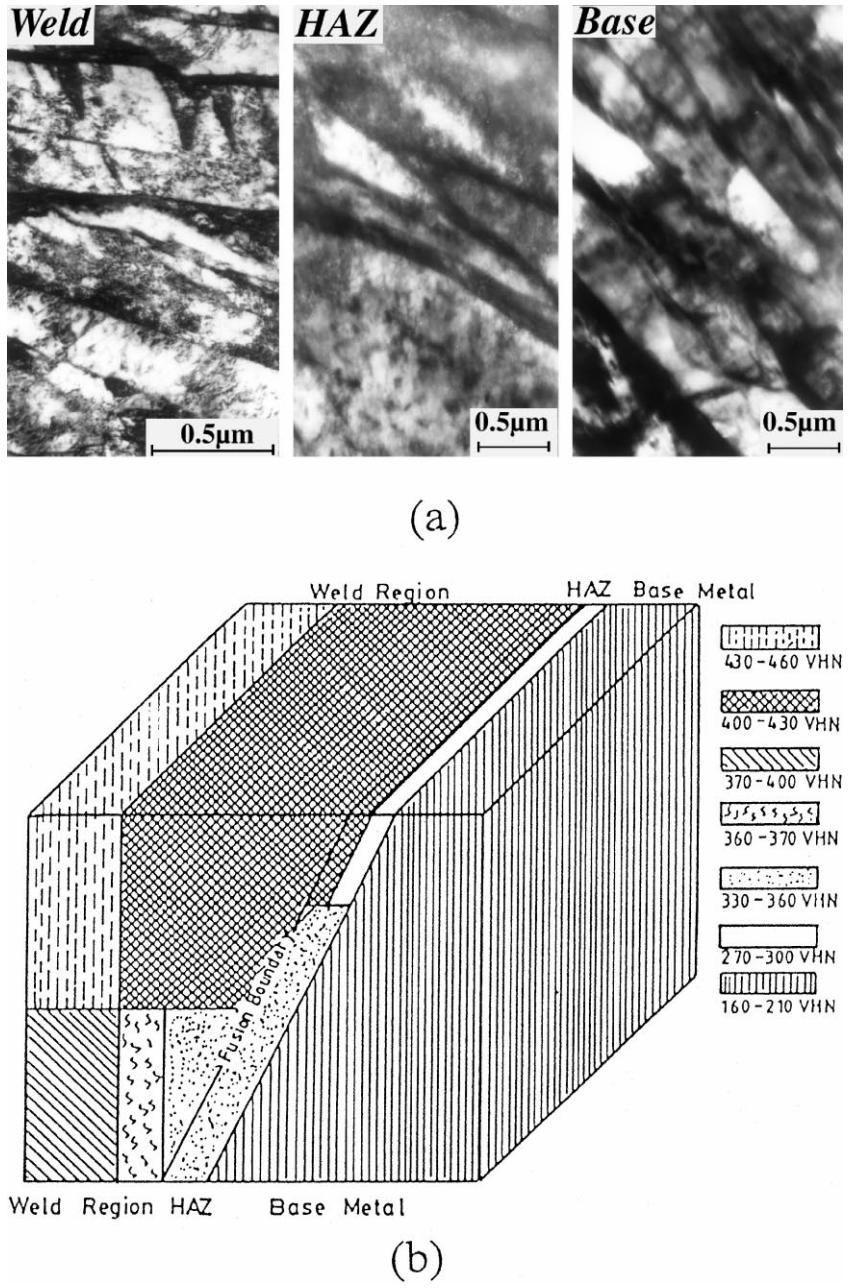

Fig. 1. (a) Microstructures of the three different zones of the weldment of 9Cr–1Mo steel. (b) Representation of the variation in hardness across different zones.

Fig. 4(a) shows the micrograph of the weld region tempered at 1023 K for 2 h. The formation of subgrains can be seen indicating the process of recovery. Fig. 4(b)–(d) shows the micrographs of the carbon extraction replica of the three regions, the weld, the HAZ and the base metal, of the same weldment. The carbides are found to be along the subgrain boundaries, suggesting a significant degree of recovery and precipitation. There is extensive precipitation of carbides, since 1023 K happens to be the nose of the TTT diagram, for the precipitation of $M_{23}C_6$ carbides.

Exposure to 1223 K has led to an additional mode of softening, i.e., the precipitation of proeutectoid ferrite (α), as can be seen in Fig. 5. The observations on the

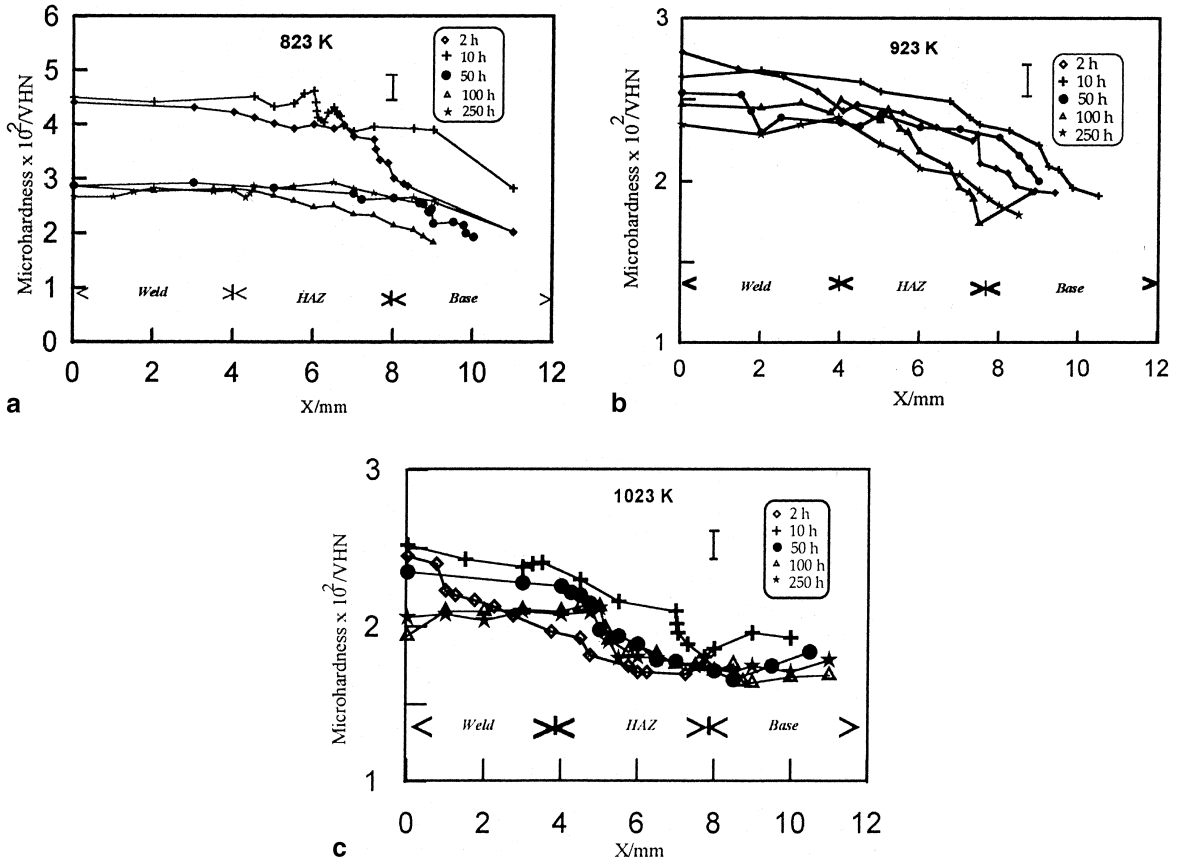

Fig. 2. Variation of microhardness with distance, x, from the weld centre line. The weldments of 9Cr–1Mo steel have been tempered at (a) 823, (b) 923 and (c) 1023 K, for different durations.

carbon extraction replica of these samples suggested that there were no carbides in any of the weldments tempered at 1223 K, due to complete dissolution of all the pre-existing carbides.

Based on the microstructural studies of the various regions of the weldment exposed to elevated temperatures, three distinct mechanisms could be identified for the gradual softening observed in the weldments. The softening at low temperatures is due to the precipitation of carbides, retaining the lath structure of the parent martensite (α'), whereas, at medium temperatures, the recovery and recrystallisation of the lath structure, proceed to considerable extent, along with precipitation. At temperatures between A_{c3} and A_{c1}, the third factor, namely the growth of soft α-ferrite is the operative mechanism. In the present study, choice of high temperatures is useful for the identification of the tempering mechanisms. However, the commercial practice of tempering is confined to temperatures less than 1023 K. The classification of tempering processes, similar to those described above have been reported [9,10] in earlier studies also. The results of the present study, support the following classification of the softening mechanisms:

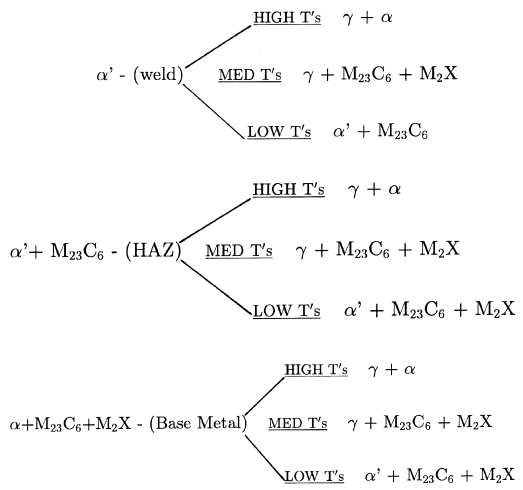

3.2. Tempering kinetics

The operative mechanism that contributes to the softening process is found to be characteristic of the

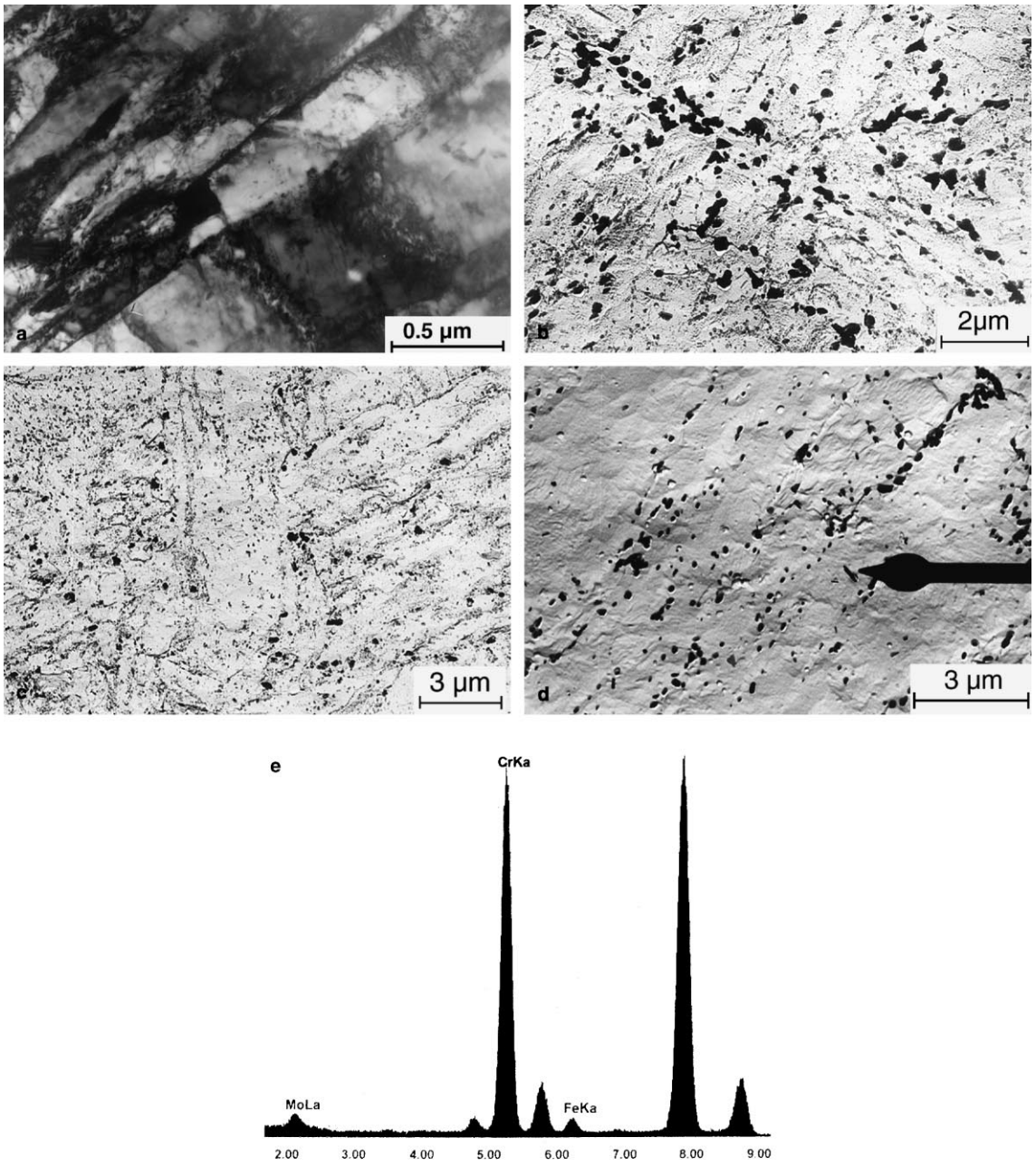

Fig. 3. Microstructural evidence for the tempering process at 823 K after 250 h. (a) Weld, (b)–(d) carbon extraction replica of weld (b), HAZ (c) and base metal (d), (e) EDAX spectrum of carbide arrow marked in (d). Retention of lath structure is seen in addition to precipitation of fine carbides along the lath boundaries. Cr rich M_2X (e) in the base metal is characteristic of the initial microstructure of the normalised and tempered 9Cr–1Mo steel.

tempering temperature. Therefore, the kinetics of tempering have been studied using any one of the regions. Of the three regions, the centre of the weld region is chosen for this purpose, due to the following reasons: high initial hardness and uniform structure within the weld zone. The heat affected zone has been avoided due to the presence of microstructurally different zones.

Fig. 6 shows the variation of hardness of the weld region as a function of tempering time, at different temperatures. The rate of softening increases with the temperature, in the range 823–1023 K, while at 1223 K,

there is a significant deviation. At 1223 K, there is a small, rapid reduction in hardness initially, followed by a high saturation value of hardness. The formation of proeutectoid α-ferrite and the decomposition of remaining γ to α' are responsible for the above observations. The tempering kinetics at the other three temperatures follow a similar behaviour: lower saturation hardness at higher temperatures and timings and less time to reach saturation hardness at higher tempering temperature. Therefore, the tempering kinetics were studied using the data at these three temperatures. In order to verify if the kinetics of tempering follow an Arrhenius behaviour and to identify the underlying operative mechanism of the tempering processes, the temperature dependence of the appropriate kinetic parameter has been studied.

In the present case, the recovery rate, i.e., the variation of hardness in a given time interval, has been chosen as the appropriate kinetic parameter. Fig. 6 shows that the hardness at any temperature reduces rapidly initially, followed by a saturation. This suggests that most of the tempering is complete within few hours of tempering and thereafter, recovery is negligible. Hence, the initial portion of each of the curves in Fig. 6 is fitted to a straight line and its slope calculated. The values of the slope of these lines, the kinetic parameter at the three temperatures of interest, are listed in Table 3. The temperature dependence of this parameter, i.e., the recovery rate, is studied. An Arrhenius plot, variation of log(recovery rate) vs $(1/T)$ is shown in Fig. 7. The linear behaviour with a negative slope suggests that the process follows an Arrhenius behaviour. The steep nature of the line, suggesting a high value of the slope, implies that the rate controlling step has a very low activation energy. The apparent activation energy, calculated based on Fig. 7 is around 0.63 eV. This value compares very well with the value [11] of interstitial diffusion of carbon in α-ferrite (80 kJ/mol), which is 0.83 eV. Therefore, it is reasonable to conclude that the rate limiting step in the tempering kinetics of the weld is the interstitial diffusion of carbon.

4. Summary

The paper presents the microstructural mechanisms and the kinetics of tempering of the weldment of 9Cr–1Mo steel. A classification scheme is proposed to explain

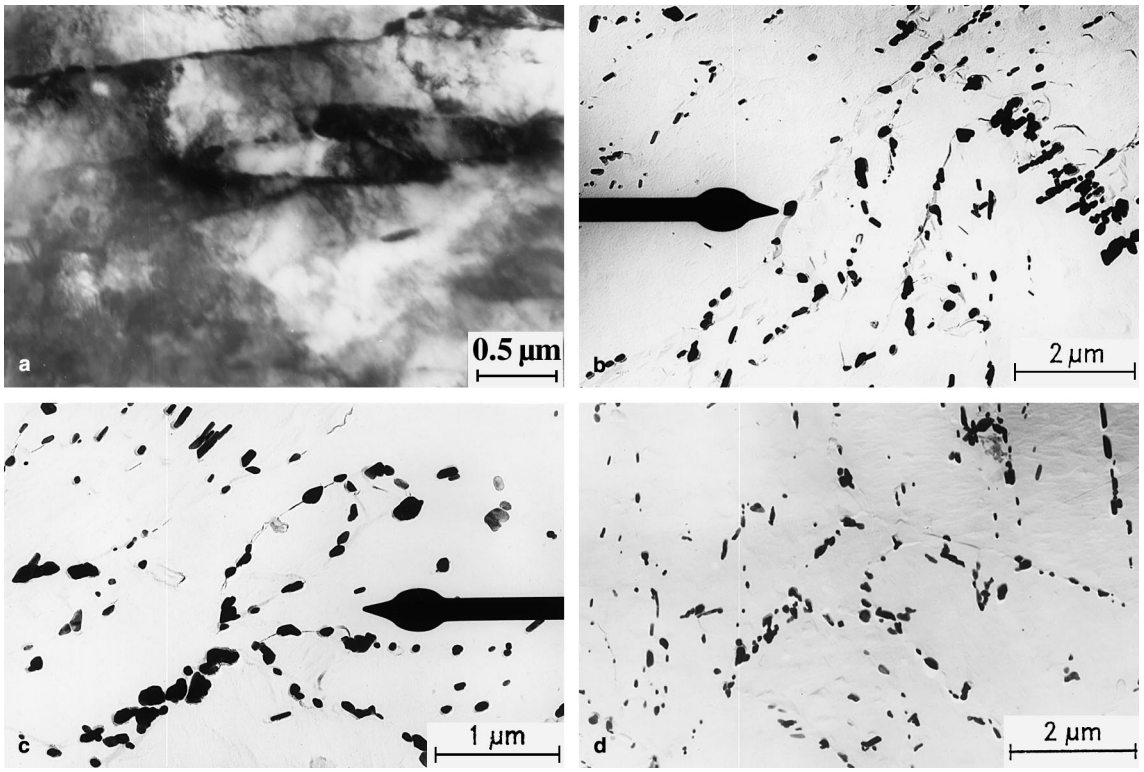

Fig. 4. Microstructural evidence for the tempering process at 1023 K for 2 h. (a), (b) Weld, (c) HAZ and (d) base metal. A significant degree of recovery, with carbides along the subgrain boundaries is seen. The arrow-marks in (b) and (c) show the carbides from which Cr rich EDAX spectra, characteristic of M_2X, were obtained. Formation of M_2X is characteristic of the exposure to high temperature.

the temperature dependence of the tempering processes, in the different zones of the weldment of 9Cr–1Mo steel. The activation energy for the tempering process has been evaluated as ≈ 0.63 eV. This value compares reasonably well with the activation energy of 0.8 eV for migration of carbon in α-ferrite. Hence, it can be

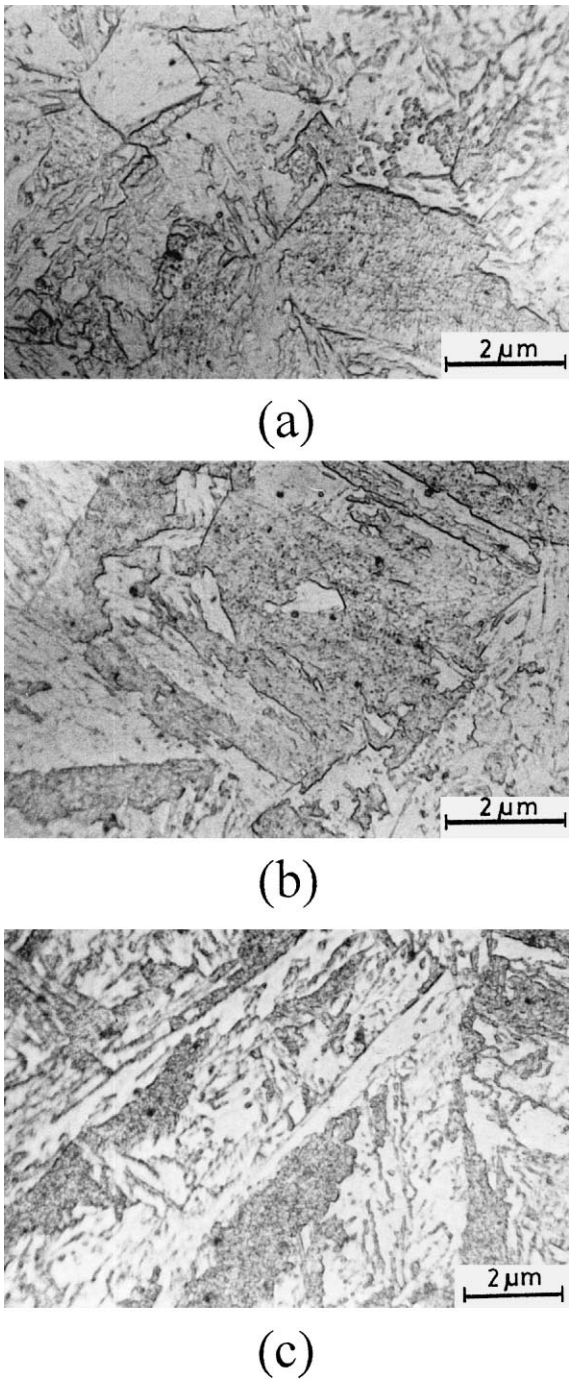

Fig. 5. Formation of pro-eutectoid ferrite (α) in the martensitic (α′) matrix is seen in the weldment aged at 1223 K for 500 h. (a) Weld, (b) HAZ and (c) base metal.

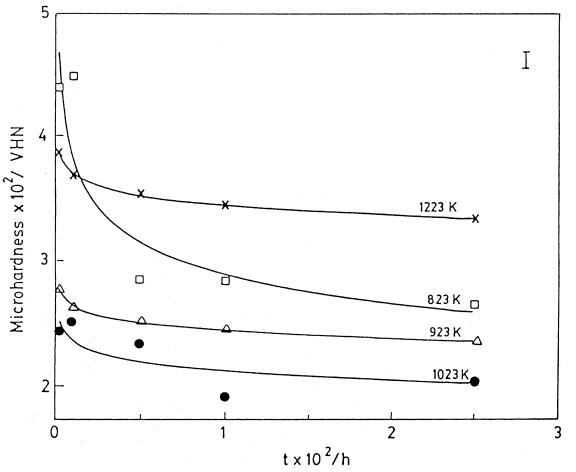

Fig. 6. Variation of microhardness (load = 100 g) of the weld region with time at various temperatures.

Table 3
Recovery rate of weld region of 9Cr–1Mo weldment at high temperatures

Sl. no.	Temperature (K)	Recovery rate (ΔVHN/Δt)
1	823	1.44
2	923	2.24
3	1023	2.84

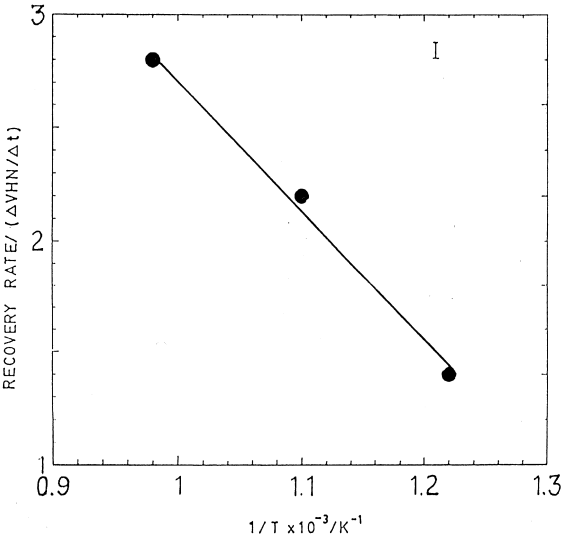

Fig. 7. Arrhenius plot of the rate of recovery of weld region of 9Cr–1Mo weldment.

concluded that the migration of interstitial carbon in α-ferrite is the rate limiting step for the tempering process.

Acknowledgements

The authors have great pleasure in acknowledging the constant support and the keen interest provided by Dr Baldev Raj, Director, Metallurgy and Materials Group and Dr Placid Rodriguez, Director, IGCAR.

References

[1] E.A. Little, in: Proceedings of the International Conference on Materials for Nuclear Reactor Core Applications, vol. 2, Bristol, October 1987, p. 47.
[2] J. Orr, F.R. Beckitt, G.D. Fawks, in: S.F. Pugh, E.A. Little (Eds.), Proceedings of the International Conference on Ferritic Steels for Fast Reactor Steam Generators, BNES, London, 1978, p. 91.
[3] M.K. Brooker, V.K. Sikka, B.L.P. Booker, in: A. Khare (Ed.), Proceedings of the International Conference on Production, Fabrication, Properties and Applications of Ferritic Steels for High Temperature Applications, ASM, Metals Park, OH, 1982, p. 257.
[4] S.J. Sanderson, in: A. Khare (Ed.), Proceedings of the International Conference on Production, Fabrication, Properties and Applications of Ferritic Steels for High Temperature Applications, ASM, Metals Park, OH, 1982, p. 85.
[5] M. Vijayalakshmi, PhD Thesis, University of Madras, India, August 1997.
[6] M. Vijayalakshmi, S. Saroja, V.S. Raghunathan, Scr. Mater. 41 (2) (1999) 149.
[7] M. Vijayalakshmi, S. Saroja, V. Thomas Paul, R. Mythili, V.S. Raghunathan, in: Proceedings of the International Conference on Welding and Allied Technology: Challenges in 21st Century, vol. 1, Indian Institute of Welding and Confederation of Indian Industry, New Delhi, India, February 1999, p. 585.
[8] M. Vijayalakshmi, S. Saroja, V. Thomas Paul, R. Mythili, V.S. Raghunathan, Metall. Mater. Trans. A 30 (1999) 161.
[9] F.B. Pickering, A.D. Vassiliou, Met. Technol. (1980) 409.
[10] J. Nutting, in: J.W. Davies, D.J. Michel (Eds.), Proceedings of the Topical Conference on Ferritic Alloys for use in Nuclear Energy Technologies, TMS-AIME, Pennsylvania, 1984, p. 3.
[11] V. Raghavan, Materials Science and Engineering, Prentice-Hall, New Delhi, 1984, p. 168.